

Damage Assessment through Control Feedback Expansion of Modal Space

Adam A. Cardi¹, Benjamin D. Kosbab², Timothy G. Overly³
John F. Schultze⁴, Matthew T. Bement⁵

¹ Undergraduate Student, Mechanical Engineering, Purdue University, West Lafayette, IN 47907, acardi@purdue.edu

² Senior Undergraduate Student, Civil Engineering, Rice University, Houston, Texas 77251, bkosbab@rice.edu

³ Graduate Student, Mechanical Engineering, University of Cincinnati, Cincinnati, Ohio 45221, overlytg@gmail.com

⁴ Technical Staff Member, Engineering Sciences and Applications Division, Weapon Response Group, Los Alamos National Lab, Los Alamos, New Mexico, schultze@lanl.gov

⁵ Technical Staff Member, Engineering Sciences and Applications Division, Directors Office, Los Alamos National Lab, Los Alamos, New Mexico, bement@lanl.gov

ABSTRACT

Damage assessment is often done through correlating changes in a system's modal properties. In this research, the modal space is expanded through adding known virtual changes to the system dynamics at discrete points. This is the control feedback process is similar in principle to the Perturbed Boundary Condition methods that were proposed in the previous decade but more expansive through choice of controller parameters. By assembling these perturbed systems in concert with the baseline model the system space is expanded and changes in modal properties can be more readily observed. From these changes, inferences about physical alterations of the system can be deduced. Specifically, this project will assess the degree to which the technique proposed in [3] is applicable to a real structure, with the ultimate goal of identifying the location and level of structural change to a cantilever beam.

NOMENCLATURE

M	Mass matrix
K	Stiffness matrix
D	Damping matrix
C_a	Controller acceleration influence matrix
C_v	Controller velocity influence matrix
C_d	Controller displacement influence matrix
n	Number of natural frequencies
r	Number of damage variables
m	Number of controller gains

1. INTRODUCTION

A reliable and efficient method for structural damage detection would effectively increase a structure's life span. Damage in this context can be considered as changes in a system that adversely affects the current or future performance of that system. The ability to detect damage could enable the switch from time-based maintenance to condition-based maintenance, thereby reducing cost and increasing reliability. With the knowledge about location and extent of damage, one could make necessary repairs before failure occurs rather than use scheduled maintenance techniques. Damage detection therefore could lower maintenance costs, increase a structure's safety, as well as increase service life.

In the past, many damage detection techniques have been successfully implemented. While visual cues are often used, this requires an unobstructed view of the structure in question. Other techniques such as acoustic, ultrasonic, eddy-current, and radiograph methods require that the damage location is already known, and that access to that location is readily available [1]. Because of these limitations, a global damage detection method has been heavily sought.

Many consider vibration-based damage detection methods to be a viable method for structural health monitoring, and has been heavily researched in recent years [2]. The idea behind vibration-based testing is that damage will alter the system's mass, stiffness, or energy dissipation properties, and therefore alter its dynamic response. A change in dynamic response from the undamaged state, in the form of mode shapes or natural frequencies, indicates a damaged structure. However, problems arise because damage is often localized, and the changes in global dynamic response are often too slight to be outside the range of test-to-test error. The information contained in the narrow band of reliable lower natural frequencies is often inadequate to detect slight system changes.

One possible solution which Lew and Juang [3] propose involves using virtual passive controllers in a closed-loop system to physically alter the natural frequencies. Lew and Juang outline an iterative algorithm that uses the observed natural frequencies of the open-loop system along with several sets of altered natural frequencies from closed-loop systems to detect structural damage. The algorithm converges to a vector of damage variables that, when compared with those of the structure in a healthy state, pinpoint and quantify damage to the structure.

The objective of this project is to experimentally verify the technique proposed and analytically verified by Lew and Juang [3]. More specifically, linear feedback control will be implemented on a cantilever beam connected to a shaker. Locating and quantifying simulated damage in the form of added mass will be attempted using the proposed method and algorithm.

2. THEORY

2.1 Direct Output Feedback

The following is some of the theory that was presented in Lew and Juang [3]:

In the case of the direct output feedback, the dynamics of the system can be described with the following two equations.

$$M\dot{x} + D\dot{x} + Kx = Bu \quad (1)$$

$$y = C_a\ddot{x} + C_v\dot{x} + C_d x \quad (2)$$

In the above Equations; M, D, and K are the Mass, Damping, and Stiffness matrices respectively. C_a , C_v , and C_d are the influence matrices for acceleration, velocity, and displacement. Also, x represents the displacement vector. In a similar manner, the equation of motion for a direct output feedback controller is shown in Equation 3.

$$u = -Fy = -FC_a\ddot{x} - FC_v\dot{x} - FC_d x \quad (3)$$

Here, u represents the input vector of controller. Then the first two equations are combined with the third to give the overall equation of motion of the system with controller. This final equation is given as:

$$(M + BFC_a)\ddot{x} - (D + BFC_v)\dot{x} - (K + BFC_d)x = 0 \quad (4)$$

This is the system that will be used to demonstrate the ability to detect damage through natural frequency shifts through the use of controllers to perturb the system. For an open loop system a set of natural frequencies can be defined; this is given in equation 5.

$$\omega_o = [\omega_{o1} \quad \omega_{o2} \quad \dots \quad \omega_{on}]^T \quad (5)$$

These frequencies correspond to the second order dynamic system previously described in Equation 1. There are n frequencies in this vector. In order to detect damage, a variable that corresponds to damage must be defined. A vector of these variables is defined in Equation 6.

$$z = [z_1 \quad z_2 \quad \dots \quad z_r]^T \quad (6)$$

Each value of z corresponds to a position on the test structure and each has a value that corresponds to percent change in the variable. A value of 1 would indicate 0% change, while a value of 1.2 would show an increase in the variable of 20%. The z variables can correspond to stiffness or mass change in the test structure. Two things should be noted about the damage variable. Firstly, the number of damage variables r can be larger than the number of natural frequencies n of the open-loop system. Secondly, the variable is called the damage variable to remain with the convention used in [3], however in this algorithm it simply corresponds to changes in mass or stiffness. Whether or not that those changes are damage, is dependant on the engineer to decide. The natural frequencies and damage variables are used in an eigenvalue problem without damping, and the general equation for the open-loop eigensolution is given in equation 7.

$$[\omega_{0i}^2 M(z) + K(z)] \phi_i = 0 \quad (7)$$

Here, i corresponds to the mode number and ϕ_i is the i^{th} mode shape. It can be seen that the mass and stiffness matrices are functions of the damage variable. In the case where the number of damage variables are larger than the number of identified natural frequencies, a closed loop system is used to augment the number of eigenvalues. The closed-loop equation is shown in 8.

$$\left[(\omega_{ci}^j)^2 M_c^j(z) + K_c^j(z) \right] \phi_i = 0 \quad (8)$$

Here, j designates the controller number, Therefore ω^j , M^j , and K^j are the natural frequencies, mass matrix, and stiffness matrix for the j^{th} controller respectively. This leads to a matrix of ω 's, one vector corresponding to each controller. If m controllers are used, the following represents the eigenvalues that would be obtained.

$$\begin{aligned} \omega_c^1 &= [\omega_{c1}^1 \quad \omega_{c2}^1 \quad \dots \quad \omega_{cn}^1]^T \\ \omega_c^2 &= [\omega_{c1}^2 \quad \omega_{c2}^2 \quad \dots \quad \omega_{cn}^2]^T \\ &\vdots \\ \omega_c^m &= [\omega_{c1}^m \quad \omega_{c2}^m \quad \dots \quad \omega_{cn}^m]^T \end{aligned} \quad (9)$$

Combining equations 9 and 5, the closed-loop and open-loop frequencies the total system natural frequencies are obtained and shown in Equation 10.

$$\omega = \left[\{\omega_o\} \quad \{\omega_c^1\} \quad \{\omega_c^2\} \quad \dots \quad \{\omega_c^m\} \right]^T \quad (10)$$

The goal of this algorithm is to determine the change in the damage variable through a change in the natural frequencies, so a sensitivity matrix for the damage variable must be computed. Equation 11 shows the sensitivity of the natural frequencies with respect to z .

$$A = \begin{bmatrix} \frac{\partial \omega_o}{\partial z_1} & \frac{\partial \omega_o}{\partial z_2} & \dots & \frac{\partial \omega_o}{\partial z_r} \\ \frac{\partial \omega_c^1}{\partial z_1} & \frac{\partial \omega_c^1}{\partial z_2} & \dots & \frac{\partial \omega_c^1}{\partial z_r} \\ & \vdots & \ddots & \\ \frac{\partial \omega_c^m}{\partial z_1} & \frac{\partial \omega_c^m}{\partial z_2} & & \frac{\partial \omega_c^m}{\partial z_r} \end{bmatrix} \quad (11)$$

The sensitivity matrix is used to calculate the change in natural frequencies from the Taylor's series expansion of the vector ω . This expansion is shown in equation 12.

$$\omega(z + \Delta z) = \omega(z) + A(z)\Delta z + \dots \quad (12)$$

If Equation 12 is linearized it can be approximated with equation 13

$$\omega(z + \Delta z) \approx \omega(z) + A(z)\Delta z \quad (13)$$

Manipulating the terms in equation 13 yields the set of linear equations expressed in equation 14.

$$A(z)\Delta z \approx \Delta \omega \quad (14)$$

This equation demonstrates that the change in damage variable can be found if the change in frequency is known, and the set of linear equations is solvable. To obtain the necessary information the following iterative steps should be followed.

1. Obtain the updated natural frequencies, $\omega(z_{new})$, by using equations 7 and 8. These will be the open- and closed-loop solutions. The initial z will be a vector of 1's equal to the length of z , this corresponds to a healthy structure.
2. Find the change in natural frequency.

$$\Delta \omega = \omega_t - \omega(z_{new}) \quad (15)$$

3. Compute the sensitivity matrix using the z_{new} .
4. Use equation 14 to compute the change in damage variable. Since the sensitivity is not a square matrix, some type of pseudo-inverse technique should be used. If absolute value of this change in damage variable is less than a predefined precision requirement, then that precision has been reached.
5. Calculate the updated damage variable.

$$z_{new} = z_{old} + \Delta z \quad (16)$$

2.2 Beam Theory

In order to successfully implement the damage detection algorithm to a cantilevered beam, an accurate finite element model needed to be created for equations 7 and 8. However, the model also needed to have clear physical meaning with respect to how each beam element was represented within the mass and stiffness matrices. The reasons for this necessity will be explained later.

An Euler-Bernoulli finite element beam model was chosen for several reasons. First, the Euler beam elements were two-dimensional, which simplified later calculations immensely. The two-dimensional Euler approximation of the cantilevered beam was acceptable [4], as evidenced by the following calculation for the aspect ratio for the beam.

$$L/t = 0.381/0.003125 > 10 \quad (17)$$

Second, clear physical understanding of how mass elements combine to form entries in the consistent mass and stiffness matrices is evidenced by the following, illustrating the assembly of two Euler beam mass elements. [5]

$$\frac{1}{420} \begin{bmatrix} 156 * m_1 & 22L * m_1 & 54 * m_1 & -13L * m_1 & 0 & 0 \\ 22L * m_1 & 4L^2 * m_1 & 13L * m_1 & -3L^2 * m_1 & 0 & 0 \\ 54 * m_1 & 13L * m_1 & 156 * m_1 + 156 * m_2 & -22L * m_1 + 22L * m_2 & 54 * m_2 & -13L * m_2 \\ -13L * m_1 & -3L^2 * m_1 & -22L * m_1 + 22L * m_2 & 4L^2 * m_1 + 4L^2 * m_2 & 13L * m_2 & -3L^2 * m_2 \\ 0 & 0 & 54 * m_2 & 13L * m_2 & 156 * m_2 & -22L * m_2 \\ 0 & 0 & -13L * m_2 & -3L^2 * m_2 & -22L * m_2 & 4L^2 * m_2 \end{bmatrix} \quad (18)$$

In this illustration, m_i is the mass of element i , and is equivalent to $\rho_i A_i L_i$; the product of the element's density, cross-sectional area, and length. Notice that where two elements overlap, at a beam node, the contributions of m_i and m_{i+1} remain discernible.

To add the contribution of damage variables, m_i is simply replaced with $z_i * m_i$. It is important to note that a change in damage variable of one element appropriately impacts the nodes to which that element contributes because there are multiple damage variables within a node. This advantage would be lost had a single damage variable been used within the entries of a node. This is the key reason and advantage for choosing these Euler beam elements.

The above argument for an Euler finite element beam model applies for stiffness matrices also. However, emphasis is on the mass matrix, as our experimental procedure involves virtual damage in the form of added mass. For this reason, our damage variable z_j correspond to mass element j .

Another reason why an Euler finite element beam model was used is evidenced by calculation of the sensitivity matrix A . As a starting point for analytically finding the sensitivity matrix of the cantilevered beam, we use

$$[K]\{\phi\}_i = \omega_i [M]\{\phi\}_i. \quad (19)$$

Here, K and M are finite element mass and stiffness matrices with ω_i and ϕ_i the i^{th} eigenvalue and mode shape. Next, we can differentiate each term with respect to the damage variables z_j , and find the relationship

$$\frac{\partial \omega_i}{\partial z_j} = \frac{\{\phi\}_i^T \left(\frac{\partial [K]}{\partial z_j} - \omega_i \frac{\partial [M]}{\partial z_j} \right) \{\phi\}_i}{\{\phi\}_i^T [M] \{\phi\}_i * 2\omega_i}. \quad (20)$$

This partial derivative in fact represents $A(i,j)$, the sensitivity of natural frequency i to a change in damage variable j . Due to the nature of the Euler finite element beam model, computation of $\partial [M] / \partial z_j$ and $\partial [K] / \partial z_j$ become very simple. In the case of a cantilevered beam with mass damage variables, $\partial [K] / \partial z_j$ becomes zero.

Calculation of $\partial [M] / \partial z_j$ is only slightly more complicated. The partial derivative is in fact a matrix of size M but with zeros except at the 4x4 mass element j , where the Euler beam element remains, but without the z_j term, lost as a result of differentiation with respect to z_j .

While other finite element beam models could also be implemented, as an initial test of the analytic algorithm, the simplicity of the Euler beam model proves beneficial for the above reasons. It is essential that physical meaning remains in the mass matrix, and that individual elements and nodes can be distinguished.

2.3 Controller Implementation

Direct feedback acceleration proportional control [3,6,7] was implemented in order to shift the natural frequencies of the cantilevered beam to increase the modal space. Acceleration was a measured state, and the use of any other states would require an observer that would inevitably add phase to the system. The control force was exerted on the beam via an electrodynamic shaker with a relatively flexible stinger in order to minimize coupling.

As it relates to the Euler finite element beam model, a control gain can be thought of as effectively adding a constant to an entry into the mass matrix. More specifically, the control gain acts as mass added to a translation node. Mathematically, a mass matrix with a control gain c applied at the node joining element 1 and 2 would appear as follows

$$\frac{1}{420} \begin{bmatrix} 156 * m_1 & 22L * m_1 & 54 * m_1 & -13L * m_1 & 0 & 0 \\ 22L * m_1 & 4L^2 * m_1 & 13L * m_1 & -3L^2 * m_1 & 0 & 0 \\ 54 * m_1 & 13L * m_1 & 156 * m_1 + 156 * m_2 + c & -22L * m_1 + 22L * m_2 & 54 * m_2 & -13L * m_2 \\ -13L * m_1 & -3L^2 * m_1 & -22L * m_1 + 22L * m_2 & 4L^2 * m_1 + 4L^2 * m_2 & 13L * m_2 & -3L^2 * m_2 \\ 0 & 0 & 54 * m_2 & 13L * m_2 & 156 * m_2 & -22L * m_2 \\ 0 & 0 & -13L * m_2 & -3L^2 * m_2 & -22L * m_2 & 4L^2 * m_2 \end{bmatrix} \quad (21)$$

Because the control gain c does not have a corresponding damage variable, it does not appear in the $\partial [M] / \partial z_j$. This fact could pose potential problems, as each set of n rows of the sensitivity matrix are therefore only different due to the λ_i and ϕ_i terms of each entry. Without proper control gain selection [8,9], the sensitivity matrix can be more ill-conditioned than current mathematical procedures can compensate for, resulting in an unsolvable set of linear equations.

Acceleration feedback control is limited in its ability to significantly shift the natural frequencies of a system because the resulting system transfer function is one that has the same order polynomial in the numerator and the denominator. Consequently the natural frequencies are less sensitive to changes in controller gain. It was observed that the experimentally implemented system went unstable due to phase lag with a gain of 0.012 applied to the feedback of the acceleration measured by the accelerometer closest to the cantilevered end. Due to time constraints and an inherent sensitivity to noise in the aforementioned damage detection algorithm (discussed later), there were no further attempts to alleviate this issue.

It was observed that the effective gain exerted on the beam, although specified as a constant in the FE model, varies with frequency as shown below in Figure 2.1.

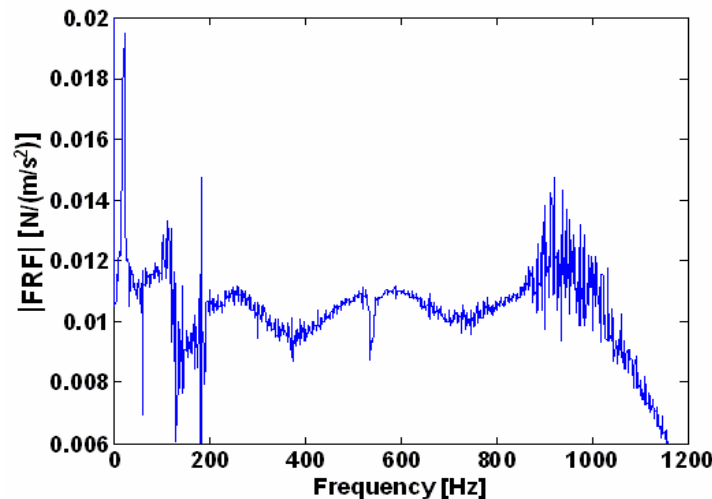


Figure 2.1: The controller gain vs. frequency.

If direct feedback control were to be implemented, it is critical that the effective gain in the system be known. Therefore the Fast Fourier Transform (FFT) of the control signal going to the shaker could be multiplied by the inverse of the Frequency Response Function (FRF) shown above in Figure 2.1 in order to account for the interactions with the beam and shaker dynamics. However, this would introduce further issues when detecting damage in the beam because this FRF is based on an undamaged case.

Due to time constraints, perfecting the controller became a second priority. Perturbing the system enough to shift the natural frequencies was done with a simulated controller in the form of added mass. In this way, we have a measurable control gain.

3. TEST SETUPS

The following is a list of the applicable devices that were used in various parts of the experimentation.

1. National Instrument Computer/Data Acquisition: NI PXI-1042Q
2. National Instruments Signal Conditioner: SC-2345
3. Dactron Spectrabook
4. PCB Piezotronics Sensor Signal Conditioner: 481
5. PCB Piezotronics Accelerometers: 352C22
6. PCB Piezotronics Hand Calibrator: 394C06
7. PCB Piezotronics Load Cell: 208C03
8. PCB Piezotronics Hammer: 084A14
9. PCB Piezotronics Hammer Load Cell: 086D80
10. Labworks Amplifier: PA-119
11. Labworks Shaker: ET 132-203
12. Isotron Accelerometers: 2250A-10

The test specimen for this experiment was a 15 in aluminum cantilever beam that was controlled through acceleration feedback. A picture of this beam is shown in Figure 3.1. The devices from the previous list that appear in this photograph are labeled.

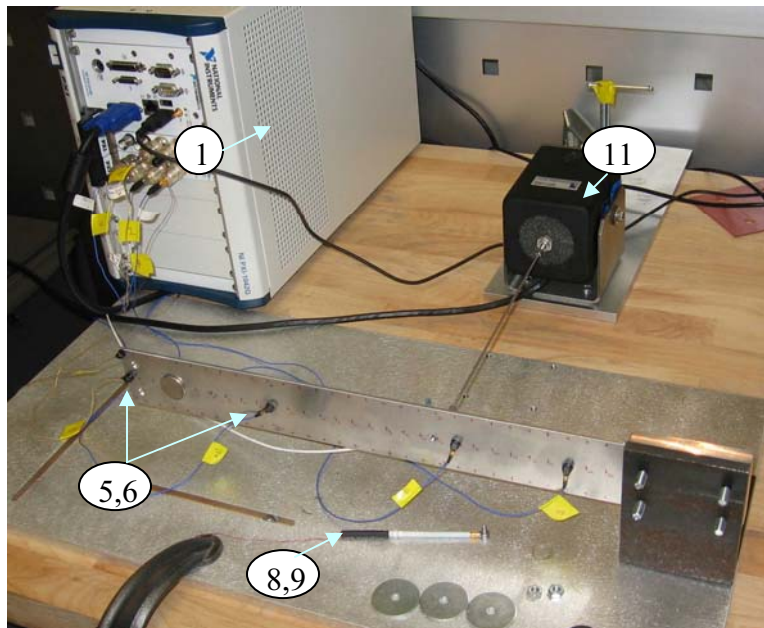


Figure 3.1: Primary feedback control test setup with cantilever beam and shaker

There were four main setups for the experiment. There were two systems used for modal parameter estimation and two used for modal space expansion. The first two setups were used to obtain and or verify the modal characteristics of the cantilever beam system. These two testing arrangements are shown in Figure 3.2

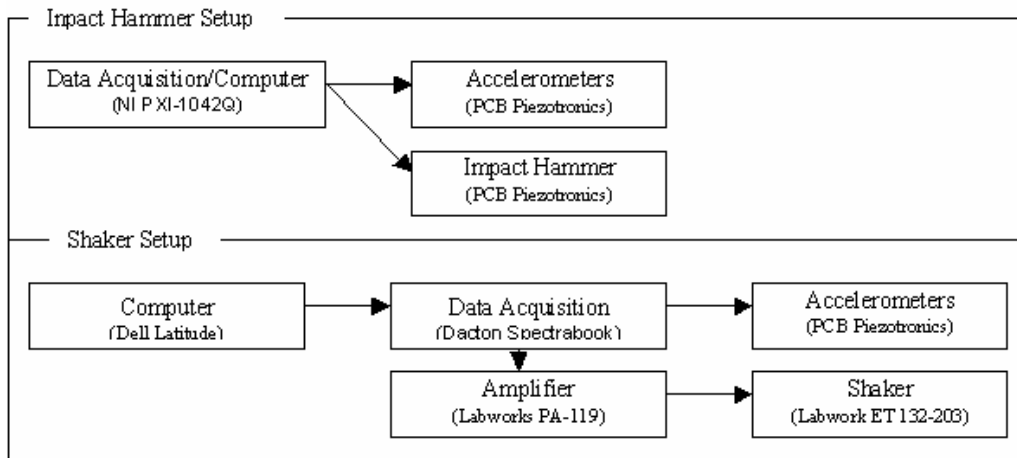


Figure 3.2: Modal identification test setups for impact hammer and shaker excitation.

In the modal identification tests in Figure 3.2, impact hammer and shaker excitation are shown. In the impact hammer configuration, depending on the experiment that was being run, the shaker may or may not have been attached. However, it was not used for excitation, so is not shown in the Figure 3.2.

The final two setups were the modal space expansion systems. The first setup was the actively controlled system. This arrangement was used to obtain sets of natural frequencies, and is shown in Figure 3.3.

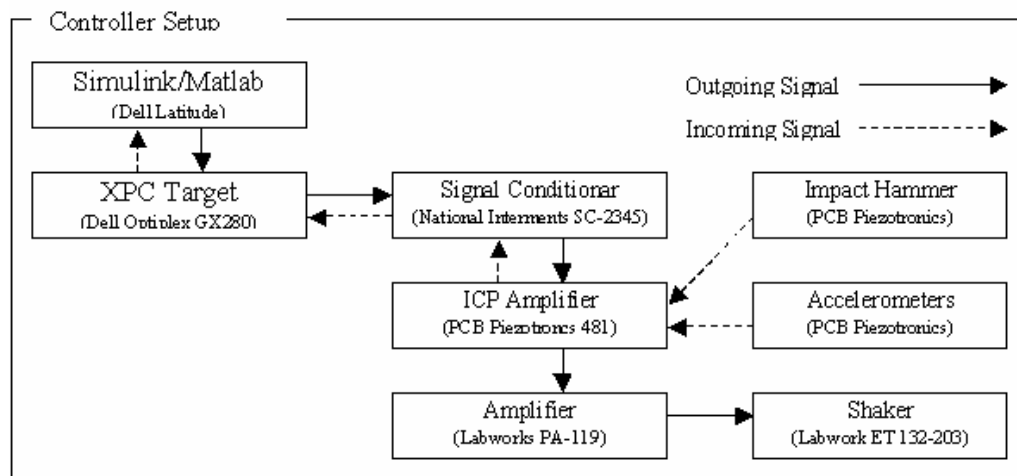


Figure 3.3: The test setup with the acceleration feedback controller

In this system, the impact hammer was used for excitation and the accelerometers were used for the feedback signal that in turn drove the shaker to provide the control. In this arrangement, the following procedure was used:

1. The controller was loaded from Simulink to the XPC target.
 - a. Once the controller was activated, energy was imparted to the beam through the impact hammer.
 - b. The controller actively added acceleration feedback to the system, and the data was recorded.
 - c. Five averages were obtained by repeating a and b.

2. The effective gain on the controller was changed and step one was repeated a total of five times for the necessary sets of natural frequencies.
3. The Frequency Response Functions of the recorded time histories were computed.
4. The natural frequencies of the five systems were identified.

The second modal expansion system was a modification of the actively controlled system. This setup was used to simulate the controller though physically adding mass. This was done due to the stability issues that were described in Section 2. The setup was identical to the Impact Test Setup from Fig 3.2 with the addition of mass to the location of the stinger attachment. The following procedure was used in the modified system.

1. The specific gain (physical mass) was added to the beam at the point of stinger attachment.
 - a. Five averages were taken using the NI Data Acquisition system.
2. The gain was changed and step one was repeated a total of five times for the necessary sets of natural frequencies.
3. The Frequency Response Functions of the recorded time histories were computed.
4. The natural frequencies of the five systems were identified.

4. RESULTS

To test the validity of our algorithm, several theoretical damage cases similar to those in [3] were calculated and presented here. The following table (4.1) shows how the damage variables converge for a 15 element beam with small damage in elements 5, 8, and 11.

Iteration #	1	True
Damage variable		
1	1	1
2	1	1
3	1	1
4	1	1
5	0.998	0.998
6	1	1
7	1	1
8	0.998	0.998
9	1	1
10	1	1
11	0.998	0.998
12	1	1
13	1	1
14	1	1
15	1	1

Table 4.1: Algorithm convergence for small damage case

It can be seen that the algorithm converges in 1 iteration. The damage variable in this case applies to changes in mass of the element. Table 4.2 confirms that a relatively large amount of damage can also be detected.

Iteration #	1	2	3	4	True
Damage variable					
1	1.23	1.10	0.99	1.00	1.00
2	0.80	0.80	0.69	0.70	0.70
3	1.22	1.06	1.00	1.00	1.00
4	0.45	0.58	0.60	0.60	0.60
5	0.79	0.80	0.80	0.80	0.80
6	0.81	0.92	1.00	1.00	1.00
7	0.90	0.94	0.99	1.00	1.00
8	0.50	0.65	0.70	0.70	0.70
9	0.92	0.96	1.00	1.00	1.00
10	1.01	1.00	1.00	1.00	1.00
11	0.66	0.76	0.80	0.80	0.80
12	1.06	1.05	1.00	1.00	1.00
13	0.96	0.93	1.00	1.00	1.00
14	0.61	0.73	0.60	0.60	0.60
15	0.24	0.07	1.07	1.01	1.00

Table 4.2: Algorithm convergence for large damage case

For the case with a 30% damage in element 2 and 8, 40% damage in element 4 and 14, and a 20% damage in elements 5 and 11, convergence to the true state occurred in 4 iterations. For both analytic example cases, five closed-loop systems with control gains of [0.01 0.02 0.03 0.04 0.05 0.06] (kg) were used along with the open-loop system.

After obtaining the natural frequencies of the experimental acceleration feedback system from the procedure outlined in Section 3, we concluded that there was no measurable shift in natural frequencies of the system, prior to instability. This was possibly due to phase lag or lag of shaker power. However, with simulated controllers with gains of [0 0.00666 0.02609 0.04552 0.06495 0.08438] (kg), frequencies shifted noticeably. Table 4.3 and 4.4 show the frequencies of the experiment and FE predictions, respectively.

Control Gain(kg)	0	0.00666	0.02609	0.04552
Mode 1	17.337	17.3	17.194	17.089
Mode 2	108.56	105.72	98.43	92.379
Mode 3	303.44	292.33	270.37	257.14
Mode 4	597.23	595.47	592.13	590.18
Mode 5	985.64	969.62	938.29	920.13
Mode 6	1470.6	1427	1362.8	1334.6
Mode 7	2064.7	2059.4	2051.5	2047.8
Mode 8	2747.6	2705.9	2639.4	2608.5

Table 4.3: natural frequencies (Hz) of experimental system with added mass controller

Control Gain(kg)	0	0.00666	0.02609	0.04552
Mode 1	16.724	16.697	16.625	16.581
Mode 2	105.23	102.45	94.979	89.727
Mode 3	292.53	284.28	267.2	257.74
Mode 4	589.53	587.26	581.4	575.67
Mode 5	959.19	942.21	911.8	900
Mode 6	1419.9	1393.8	1353.8	1333.1
Mode 7	1962.1	1950.7	1908.6	1859.7
Mode 8	2712.2	2665.8	2605	2573.3

Table 4.4: natural frequencies (Hz) of FE system with added mass controller

It is apparent that, while not perfect, the FE system predicts the shifts in natural frequencies to a reasonable degree: within approximately ~2%. However, when the experimental frequencies are input to the algorithm as a damaged state in order to find a baseline damage vector, the algorithm does not converge, or converges to a damage vector beyond physical feasibility. With a simulated damage case of added mass (both on the open-loop and closes-loop systems), the algorithm will not converge to the added mass.

5. DISCUSSION

After determining convergence would not occur with our experimental results, several aspects of the damage detection algorithm were examined. This was done to determine that if a small error in natural frequencies could

be achieved, would the algorithm be robust enough to detect the damage and if not, what could be done to solve the problem.

The first aspect assessed was the ability of the algorithm to handle errors in the measured natural frequencies. Adding a 0.5% maximum random error to the theoretical natural frequencies of the system performed this verification. With this frequency perturbation, the algorithm converged to a damaged state well beyond 0.5% damage. Figure 5.1 shows convergences for the theoretically perturbed frequencies.

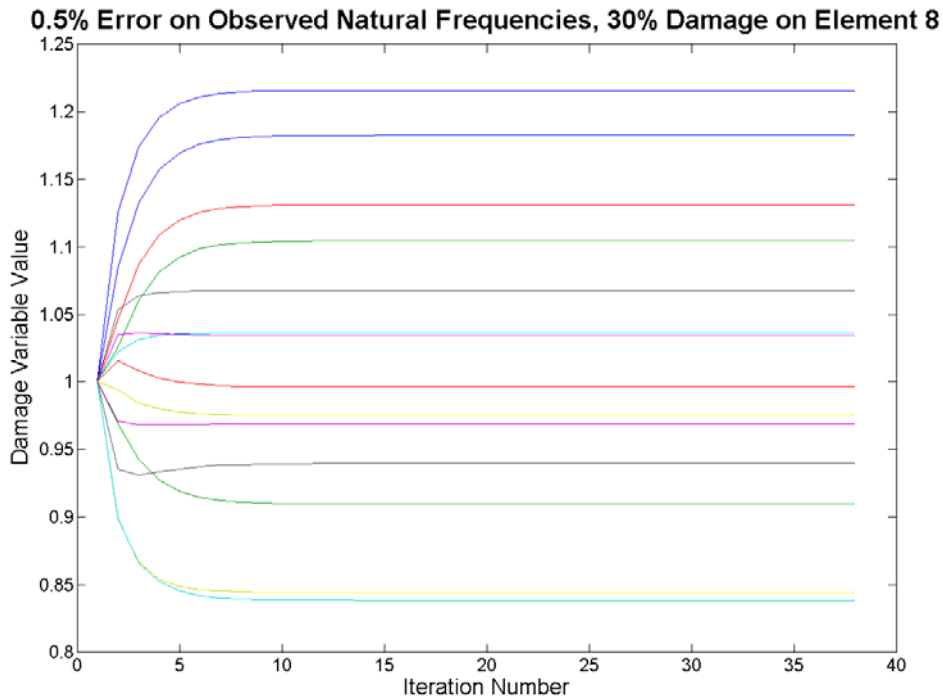


Figure 5.1: Converged damage case with 0.5% random error on the inputted natural frequencies

The fact that a small frequency perturbation changes the convergence of the algorithm to such a large degree can be explained by the fact that natural frequencies in the band of interest are inherently insensitive to small, local changes of mass. Therefore, any small error in recorded experimental natural frequencies will be amplified to errors in computed damage. Often times, this amplification pushed the artificially computed damage beyond the window of true damage for which one would be monitoring. This is also demonstrated in Fig. 5.1, where the element with the 30% mass increase cannot be verified. In fact, the range of artificially computed error changes, depending on which elements in the structure have the error. Fig. 5.2 shows a plot of possible computed damages based on different errors introduced to theoretically determined natural frequencies.

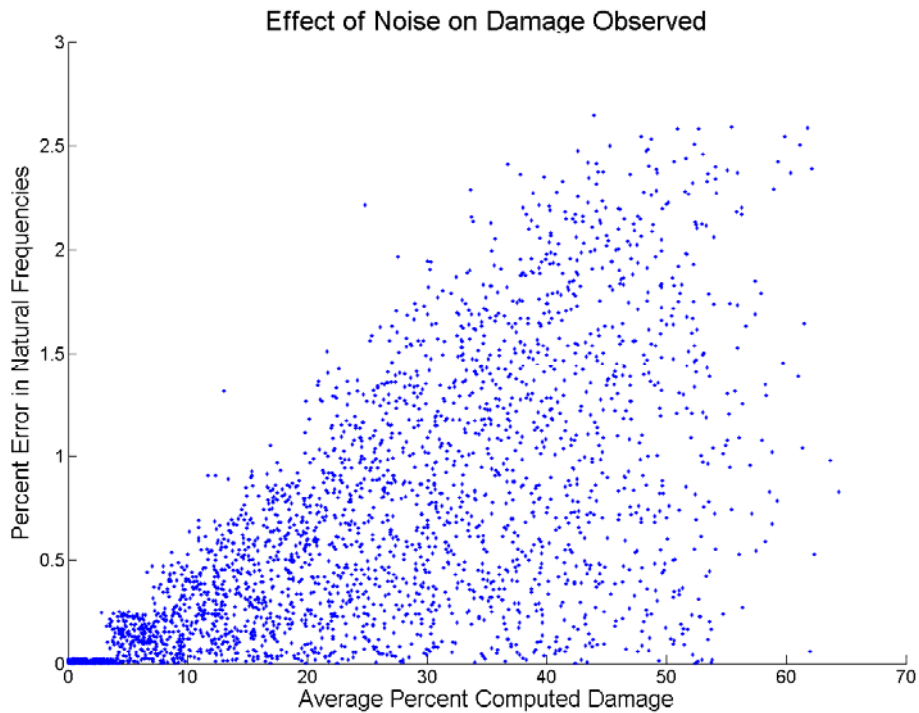


Figure 5.2: Possible errors in damage due to errors in natural frequencies.

Fig 5.2 shows the large variance in computed damage that was seen with small amounts of error in the natural frequencies. Depending on, where the error is applied and how great that error is, leads to this great difference in computed damage. It can be seen, for example, that a 0.5% average random error applied to the beam would result in between approximately 10% and 60% computed damage. Meaning, with even a random error of this magnitude, the damage would have to be of approximately 60% or greater to be detected. As the algorithm stands, bias errors over approximately 1% do not allow for convergence to a solution, and even a smaller random error is acceptable.

Several changes to the algorithm may enhance its ability to deal with measurement error. Damage variables may respond more effectively if related to stiffness, as opposed to mass. Also, a different model for the system would be needed. It appears that the Euler-Bernoulli model for the beam alone is too simple to model the system accurately enough to be a final model. The entire system; shaker, boundary condition, stinger, etc. need to be modeled for more effective damage detection. Also, a second-order dynamic controller, as proposed in [3], may prove to be a more effective method for expanding modal space information. Using a genetic algorithm, or other minimization technique, may be beneficial; with such, one may not need a sensitivity matrix, and would therefore avoid many mathematical issues. However, this would also be ignoring the advantage of information contained within the sensitivity matrix.

Using control feedback to expand modal space information is a promising technique for extracting more information from the same frequency band. It would be extraordinarily useful, as detection resolution could be higher than current methods, and with a moderate number of sensors. However, the difficulty of perfect modeling and measuring natural frequencies obstructs this goal. As it stands, experimental implementation of the method proposed in [3] is very practically challenging.

6. REFERENCES

- [1] Doebling, S. W., Farrar, C. R., Prime, M. B., and Shevitz, D. W., "A Review of Damage Identification Methods that Examine Changes in Dynamic Properties," *Shock and Vibration Digest* 30 (2), pp. 91-105, 1998.

- [2] Bement, M. T. and Farrar, C.R., "Issues for the Application of Statistical Models in Damage Detection," Proceedings of IMAC-XVIII, the 18th International Modal Analysis Conference, Feb. 7-10, 2000, Texas, p. 1392.
- [3] Lew, J.-S., Juang, J.-N., "Structural Damage Detection Using Virtual Passive Controllers," *Journal of Guidance, Control, and Dynamics*, Vol. 25, No. 3, 2002, pp. 419-424.
- [4] [Adams, R. D. and Bacon, D. G. C., Measurement of the flexural damping capacity and dynamic Young's modulus of metals and reinforced plastics, *Journal of Physics D: Applied Physics*, 6 (1973), pp. 27—41.
- [5] Cook, R.D, *Concepts and Applications of Finite Element Analysis*, Second Edition, New York: Wiley, 1981.
- [6] Juang, J.-N. and Phan, M., "Robust Controller Designs for Second-Order Dynamic Systems: A Virtual Passive Approach," *Journal of Guidance, Control, and Dynamics*, Vol. 15, No. 5, 1992, pp. 1192-1198.
- [7] Chuang, C.-H., Courouge, O., and Juang, J.-N., "A Robust Controller for Second-Order Systems Using Acceleration Measurement," *Journal of Dynamic Systems, Measurement, and Control*, Vol. 119, No. 2, 1997, pp. 350-354.
- [8] Ray, L.R., Tian, L., "Damage Detection in Smart Structures through Sensitivity Enhancing Feedback Control," *Journal of Sound and Vibration*, Vol. 227, No. 5, 1999, pp. 987-1002.
- [9] Okubo, N., Toi, T., "Sensitivity Analysis and its Application for Dynamic Improvement," *Sādhana*, Vol. 25, Part 3, June 2000, pp. 291-303.